Journal of Alloys and Compounds 613 (2014) 157–163

Contents lists available at ScienceDirect

Journal of Alloys and Compounds

journal homepage: www.elsevier.com/locate/jalcom

Annealing-induced shape recovery in thin film metallic glass

Alemu Tesfaye Negussie [a], Wahyu Diyatmika [a], J.P. Chu [a,*], Y.L. Shen [b], J.S.C. Jang [c], C.H. Hsueh [d]

[a] Department of Materials Science and Engineering, National Taiwan University of Science and Technology, Taipei 10607, Taiwan
[b] Department of Mechanical Engineering, University of New Mexico, Albuquerque, NM 87131, USA
[c] Department of Mechanical Engineering, National Central University, Chung-Li 32001, Taiwan
[d] Department of Materials Science and Engineering, National Taiwan University, Taipei 10617, Taiwan

ARTICLE INFO

Article history:
Received 3 May 2014
Received in revised form 5 June 2014
Accepted 6 June 2014
Available online 17 June 2014

Keywords:
Thin film metallic glass
Indentation depth recovery
Annealing
Roughness

ABSTRACT

The shape recovery property of a sputtered $Zr_{50.3}Cu_{28.1}Al_{14}Ni_{7.6}$ (in at.%) thin film metallic glass upon heating is examined. Due to the surface tension-driven viscous flow, the shape of indentation appears to recover to different extents at various temperatures and holding times. It is found that a maximum of 59.8% indentation depth recovery is achieved after annealing within the supercooled liquid region (SCLR). The amount of free volume in the film is found to play a role in the recovery. Atomic force microscopy results reveal a decrease in film roughness to a minimum value within SCLR. To elucidate the experimentally observed shape recovery, a numerical modeling has been employed. It is evident that the depressed region caused by indentation is elevated after annealing.

1. Introduction

Metallic glasses (MGs) are a type of non-crystalline (amorphous) metallic alloys lacking long-range periodicity [1–3] of the atomic arrangement. Because of their superior properties, such as absence of grain boundary, high resistance to corrosion, high strength and elastic limit [2,4,5], MGs have received much scientific and technological attention. However, extensive efforts have been given mostly for bulk metallic glasses (BMGs) [2,6–9]. For their geometrical and ductility (especially at room temperature) advantages, thin film metallic glasses (TFMGs) have evolved to be an important class of MGs for various potential applications, such as for micro- and/or nano-electromechanical systems [10].

TFMGs are considered to be free from crystalline defects, such as dislocation and grain boundaries. Because of their viscous flow in the SCLR, they are useful for miniature and complicated shape materials fabrication, as well as improvement of mechanical properties of crystalline and amorphous substrates [2,11–13]. TFMGs properties, including electrical, mechanical, and thermal properties, may alter due to variations in chemical composition, sample preparation method and temperature [14–16]. In TFMGs, annealing yields changes in these properties, particularly when the film is annealed in supercooled liquid region [SCLR, ΔT, the temperature difference between crystallization temperature (T_x) and glass transition temperature (T_g) [15–18]. This is mainly because of their low viscosity within ΔT [19,20]. Kumar and Schroers investigated the response of two different pyramidal microfeatures of BMG after annealing within ΔT. First, they imprinted pyramidal features on Pt-based BMG and then annealed within ΔT. As a result, surface smoothening is observed due to the surface tension-driven viscous flow [21]. Packard et al. also explored the influence of temperature on the response of nanoindented features of Pt-based BMG. For this case, imaging scans showed negligible change in the residual impression at temperatures below T_g, but significant recovery is observed at temperatures within SCLR [22].

A thorough knowledge about TFMG properties, including the shape recovery following contact deformation, is crucial for their potential applications. This study is thus directed to examination of the indentation recovery ability of Zr-based TFMG and effects of annealing conditions for the recovery. In addition, surface roughness of materials plays a great role in microelectronic, MEMS devices, medical devices (like microsurgical tools) [2]. Hence, in addition to the recovery, we also investigate the effect of temperature on the surface roughness of the film.

2. Experimental procedures

A Zr-based TFMG was grown on Si substrate using radio frequency magnetron sputtering system with no intentional substrate heating. The operating conditions for the sputtering system were set at base and working pressures of $\sim 5 \times 10^{-4}$ and 3 m Torr, respectively, with working distance of 10 cm in argon. X-ray energy dispersive spectrometry (EDS, Oxford X-Max) attached to scanning electron microscope (SEM, FEI QUANTA 3D FEG) was used to measure film composition. The nominal film thickness was 200 nm in all cases. Differential scanning calorimetry (DSC, Netzsch 404 F3 Pegasus) and 4-point probe (Laresta-EP MCP-T360) were used to

* Corresponding author. Tel.: +886 2 27303292.
E-mail address: jpchu@mail.ntust.edu.tw (J.P. Chu).

http://dx.doi.org/10.1016/j.jallcom.2014.06.048
0925-8388/

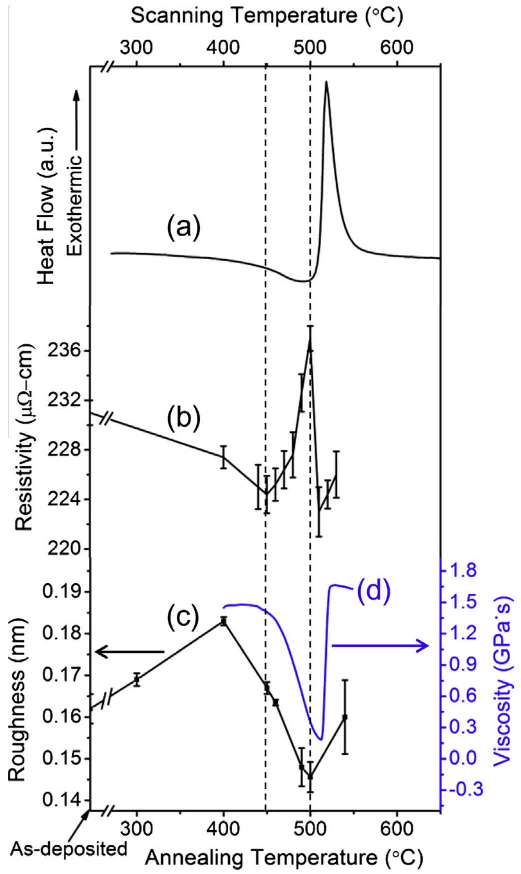

Fig. 1. (a) DSC thermogram of an as-deposited film, (b) electrical resistivity, (c) roughness of film after annealing at various temperatures, and (d) viscosity of a ribbon of similar composition as a function of temperature.

investigate the thermal and electrical properties of the film, respectively. The amorphous structure of the film in as-deposited and annealed (within ΔT) conditions were examined by the grazing-incidence X-ray diffraction (XRD, Bruker D8 DISCOVER) with monochromic Cu Kα radiation.

Nanoindentations were conducted using Hysitron TI 950 TriboIndenter with a diamond Berkovich tip. Indentations were performed in a maximum load of 195 μN using a loading rate of 65 μN/s. Samples were subjected to the atomic force microscopy (AFM, BRUKER Icon) using non-contact Scan Asyst mode in order to obtain surface topographic images and profiles. The samples were annealed at different temperatures in vacuum at $\sim 3 \times 10^{-3}$ m Torr. Viscosity measurement was performed using dynamic mechanical analyzer (DMA, TA Instruments DMA 2980). The finite element program ABAQUS (Dassault Systemes Simulia Corp., Providence, RI, USA) was used for the numerical simulation.

3. Results and discussion

The chemical composition of TFMG obtained using SEM/EDS is determined to be $Zr_{50.3}Cu_{28.1}Al_{14}Ni_{7.6}$ (in at.%). Annealing of TFMGs at different temperatures yields the formation of various nanocrystalline and amorphous structures [16]. Therefore, for TFMGs, their thermal stability of the amorphous phase as a function of temperature will limit the permissible heating time and temperature during the annealing process. For this reason, determination of T_g and T_x is very crucial for thin film material properties. Fig. 1(a) and (b) shows the thermal and electrical properties of the film. The DSC result (Fig. 1(a)) shows that the amorphous film exhibits T_g, followed by a sharp exothermic peak of T_x. This phenomenon is also supported by the resistivity change of the film (Fig. 1(b)). The electrical resistivity, which is taken at room temperature after annealing at given temperatures for 1 min, decreases as the temperature increases up to 450 °C due to the stress relief and structural relaxation in the film. The annealing-induced amorphization is considered to cause the increase in resistivity between 450 and 500 °C. After 500 °C, the sharp decrease results from the crystallization. Based on these results, the T_g, T_x and ΔT values of the $Zr_{50.3}Cu_{28.1}Al_{14}Ni_{7.6}$ TFMG are determined to be 449.6 °C, 500.8 °C and 51.2 °C, respectively.

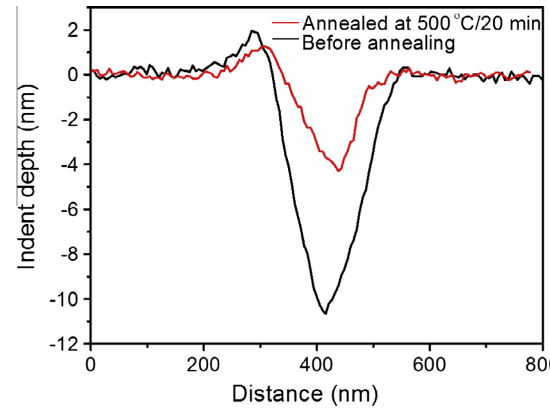

Fig. 2. AFM profiles of the indent in the film before and after annealing at 500 °C for 20 min.

Table 1
Indentation depth recovery of the film after annealing at 450, 470, 500 °C for 20 min.

Annealing temperature (°C)	Annealing time (min)	$D^b_{max} - D^a_{max}$ (nm)	D_R (in %)
450	20	5.0	50.0
470	20	5.3	54.1
500	20	6.4	59.8

Effects of annealing temperature on the surface roughness of TFMG are examined. The film roughness as a function of temperature plot is shown in Fig. 1(c). Annealing results in grain growth of nanocrystalites within the amorphous matrix when the film is annealed at temperatures below T_g and above T_x, yielding the increment of roughness. Yet, annealing within ΔT yields surface self-smoothening [2,4]. In the current work, the film roughness at temperatures 300 °C and 400 °C (both below T_g) increases from 0.162 ± 0.002 nm in as-deposited condition to 0.169 ± 0.002 and 0.183 ± 0.002 nm, respectively. This is because of grain growth or coalescence of metastable nanocrystalites in the amorphous matrix. Chou et al. [23] also reported the formation of medium range order clusters after sub-T_g annealing of the film. On the other hand, the surface becomes smoother within ΔT and the roughness is decreased to the minimum value of 0.145 ± 0.006 nm when annealed at 500 °C. This is considered due to annealing-induced amorphization and low viscosity in SCLR, which favors surface self-smoothening. Upon further annealing at 540 °C, above T_x, the film roughness increases. This is due to crystallization and grain growth. It is clearly seen that the surface roughness result is in good agreement with resistivity and DSC results.

To explore the shape recovery of the film, nanoindentations were performed and examined by AFM. The indentation depths before and after annealing are taken from the AFM measurement for comparison. Fig. 2 shows typical AFM scan profiles of an indent before and after annealing at 500 °C for 20 min. The indentation depth and profile after annealing are distinctly different from those before annealing, with a noticeable depth recovery of 59.8% from 10.7 nm to 4.3 nm after annealing. The shape recovery is obvious not only in the depth, but also in the size of indent after annealing. It is proposed that the surface tension-driven viscous flow and